



Contents lists available at SciVerse ScienceDirect

Colloids and Surfaces A: Physicochemical and Engineering Aspects

journal homepage: www.elsevier.com/locate/colsurfa



Effect of cross-link density on re-entrant melting of microgel colloids

Malte Wiemann^{a,*}, Norbert Willenbacher^b, Eckhard Bartsch^c

^a University of Freiburg, Department of Physical Chemistry, Stefan-Meier-Str. 31, 79104 Freiburg, Germany

^b Karlsruhe Institute of Technology, Department of Mechanical Process Engineering and Mechanics, Geb. 30.70, Strasse am Forum 8, 76131 Karlsruhe, Germany

^c University of Freiburg, Department of Physical Chemistry, Albertstr. 21, 79104 Freiburg, Germany

ARTICLE INFO

Article history:

Received 2 November 2011

Accepted 23 November 2011

Available online xxx

Keywords:

Microgels

Glass transition

Colloids

Re-entrant melting

Hard sphere

ABSTRACT

We investigated concentrated suspensions of newly synthesized highly cross-linked (1:10) polystyrene (PS) microgel particles dispersed in a good, iso-refractive organic solvent that allowed for a detailed study using light scattering techniques. Inducing depletion attraction by addition of non-adsorbing (PS) polymer, we analyzed the re-entrant melting behavior of the particle system. We compared our results with that of previous studies on polystyrene microgel particles with a lower cross-linking ratio (1:50) and on PMMA suspensions. In contrast to the (softer) 1:50 microgels where an unexpectedly huge re-entry effect was found with fluid samples extending up to a volume fraction $\phi \approx 0.69$, the re-entry region here extends only up to $\phi \approx 0.61$ and the attractive glass transition line is found at significantly lower polymer concentrations.

Instead we find a closer similarity of the re-entry behavior with that observed for hard sphere-like PMMA particles. Whereas the highest volume fractions up to which fluid states could be observed are comparable, the polymer concentration needed to induce re-entrant melting and the formation of attractive glass is shifted to higher polymer concentrations. While the latter effect may be attributed to the non-ideal behavior of the free polymer, the extension of the fluid region with respect to colloid volume fraction appears to depend sensitively on system details like particle softness or particle size distribution.

© 2011 Elsevier B.V. All rights reserved.

1. Introduction

Colloidal dispersions are commonly used as model systems for investigating fundamental principles of condensed-matter systems. The glass transition in particular has long been investigated with light scattering techniques using suspensions of hard sphere (HS) particles, such as sterically stabilized polymethylmethacrylate (PMMA) in cis-decalin [1–3]. The fundamental physics of the processes involved in vitrification has been successfully described within the framework of mode coupling theory (MCT) [4–6], even though some discrepancies between theory and experimental observation still remain under debate [7,8]. In addition to catching the essence of glass transition phenomena in hard sphere-like colloidal dispersions, mode coupling theory predicted the possibility of melting colloidal glasses by inducing short range attraction between the colloidal particles [6,9,10]. Attraction reduces the average distance of the particles in the suspension, freeing more

volume for particle movement and thus melting the glass. This is commonly achieved by adding non-adsorbing polymer to the colloidal suspensions, which gives rise to the so-called, well known depletion attraction [11–13]. This behavior – usually addressed as re-entrant glass transition or re-entry phenomenon – has been confirmed in several studies, using e.g. the aforementioned PMMA particles dispersed in cis-decalin [14,15] or polystyrene (PS) microgel particles dispersed in 2-ethylnaphthalene (2-EN) [16–19]. In the case of PMMA particles fluid states up to volume fractions of $\phi \approx 0.62$ were found, while it was possible to increase the fluid volume fraction up to $\phi \approx 0.69$ in the case of the PS microgel particles.

The unexpectedly large re-entry region where fluid states could be induced by adding free polymer to the colloidal glass in the case of the previously studied 1:50 cross-linked PS microgels (1 crosslink per 50 monomer units) as compared to the PMMA system raised the question to its physical origin. Even though the phase behavior, rheology, and glass transition dynamics of such microgel particles without free polymer are comparable to that of hard spheres-like colloids – such as PMMA – once an appropriate mapping of the volume fraction scale is performed [17,19], one could imagine that the discrepancies in the re-entry behavior are connected with the microgel character of the PS particles. Their inherent (slight) softness which is expressed by an inverse power interaction potential

* Corresponding author. Tel.: +49 7612036266; fax: +49 7612036306.
E-mail addresses: malte.wiemann@uni-freiburg.de (M. Wiemann), norbert.willenbacher@kit.edu (N. Willenbacher), eckhard.bartsch@physchem.uni-freiburg.de (E. Bartsch).

$u(r) \propto r^n$ with $n \approx 40$ [17] could allow some compression under the osmotic pressure exerted by the added free polymer. Moreover, in a good solvent for PS, such as 2-EN, the particles swell by a factor of $Q \approx 5$ –6. Thus it is conceivable that the particles undergo some de-swelling once free polymer is added, an effect that has been observed previously with microgel particles which, however, had a much lower degree of crosslinking ($\approx 1:200$) [20]. Besides such microgel effects which could lead to an overestimation of the colloid volume fraction, effects that lead to a more efficient packing have to be considered as well. Thus, a broad particle size distribution is known from computer simulation to shift the volume fraction of random close packing to higher values [21]. The previously studied 1:50 crosslinked microgel suspension consisted of a binary mixture particle with a size ratio $\Gamma = R_{small}/R_{large} \approx 0.8$ and a number ratio $N = N_{small}/N_{large} \approx 2.7$ amounting to an effective polydispersity of $\sigma \approx 11$ –12% ($\sigma = (\langle r^2 \rangle - \langle R \rangle^2)^{1/2} / \langle R \rangle = 0.11$ –0.12) as compared to the PMMA system where polydispersity was much smaller (< 0.07).

According to the computer simulation results such a polydispersity would shift random close packing from $\phi = 0.64$ to $\phi = 0.67$ –0.68. If this increased packing capability were supplemented with a partial ordering of particles in nanocrystalline domains under the influence of depletion forces, fluid states with packing of ≈ 0.69 might be achievable.

To elucidate the origin of the surprisingly large re-entry region of microgel colloids and to bridge the gap between the previously studied two particle systems – the PMMA particle with truly hard sphere character and the 1:50 PS microgels showing indications of softness under the influence of depletion attraction – a new system was designed with an increased cross-link ratio of 1:10 and correspondingly decreased softness. To emphasize the effects of the cross-link density on the re-entry behavior, all other characteristics of the studied 1:50 particles, such as radius in 2-EN, polydispersity, size ratio and number ratio were reproduced as closely as possible. We used dynamic light scattering to investigate the re-entrant melting behavior under the influence of depletion attraction. Here, we compare our results with the 1:10 crosslinked particle to the results on both the 1:50 microgel and the PMMA colloids.

2. Methods and materials

2.1. Dynamic light scattering (DLS)

2.1.1. Particle sizing

The dynamic light scattering experiments were performed with a He:Ne gas laser (JDS Uniphase; 1145P; $\lambda = 632.8$ nm, 22.5 mW). The sample cuvettes (VWR International Boro 3.3, 10 mm) were mounted in the vertical axis of a light-scattering goniometer (ALV/SP-86) equipped with an index match bath (Fa. ALV) and a sample holder thermostatted to 20 °C. The detection unit consisted of two Perkin Elmer photomultipliers (SPCM-CD2696 Rev.G) cross-correlated by an ALV-5000/E correlator. The scattered light was coupled via a pigtail collimator mounted on the 2nd circle of the goniometer into a monomode optical fiber (ALV) which was connected via a beam-splitting mono-mode fiber (Newport, F-CPL-S12635-FCUPC) to the photomultipliers. Using the Siegert relation [22,23] measured intensity auto-correlation functions $g_T^{(2)}(q, \tau)$

$$g_T^{(2)} = \frac{\langle I(q, t) \rangle_T \langle I(q, t + \tau) \rangle_T}{\langle I(q, t) \rangle_T^2} \quad (1)$$

were converted into the intermediate scattering functions $f(q, \tau)$ and analyzed via cumulant analysis [24]. Here T denotes the time average and q is the scattering vector (Eq. (4)). From the thus obtained diffusion coefficients the hydrodynamic radii R_H were calculated using the Stokes–Einstein equation. To acquire accurate

particle radii, the aqueous dispersions were highly diluted and the measurements of the intensity autocorrelation functions were performed over the angular range of 40–100° in steps of 1° taking one measurement of 10 min duration per angle. The calculated radii showed no dependency on the angle, indicating the absence of aggregates and a narrow size distribution. From the average of the measured radii the particle radius in aqueous suspension R_{H,H_2O} was obtained with a standard deviation of about 2%. Due to the dependence of the diffusion coefficient D_0 on the porosity – in the case of the microgels controlled by the cross-linking ratio – of the microgel particles [25], measurement of the swollen particles in the good solvent 2-ethylnaphthalene yields inherently incorrect (smaller) particle radii. Results from those measurements were only used as indication of the particle size for sample preparation for the phase behavior analysis.

2.1.2. Glass transition dynamics

The intermediate scattering function $f(q, \tau)$ contains the desired information on the particle dynamics of colloidal dispersions. This function is defined as

$$f(q, \tau) = \frac{\langle \delta\rho(q, \tau) \cdot \delta\rho(q, 0) \rangle}{\langle |\delta\rho(q, 0)|^2 \rangle}, \quad (2)$$

where

$$\delta\rho(q, t) = \int \delta\rho(\vec{r}, t) \exp[iq\vec{r}(t)] d\vec{r} \quad (3)$$

is the q th spatial Fourier component of fluctuations in the particle number density $\rho(\vec{r}, t)$ [22,23]. q denotes the magnitude of the scattering vector

$$q = |\vec{q}| = \frac{4\pi n_1}{\lambda} \sin(\theta/2) \quad (4)$$

where n_1 is the refractive index of the solvent at the wavelength λ of the light source and θ is the scattering angle. The light scattering experiments for determination of the intermediate scattering functions in the glass transition range were performed with a He:Ne gas laser (JDS Uniphase; 1145P; $\lambda = 632.8$ nm, 22.5 mW). The sample cuvettes were mounted in the vertical axis of a light-scattering goniometer (ALV/SP-125) equipped with an index match bath (Fa. ALV) and a sample holder thermostatted to 20 °C. The detection unit consisted of an ALV-SOSIP photomultiplier, and an ALV-7004 correlator. A beam-splitter directed 50% of the scattered light via a pigtail collimator mounted on the 2nd circle of the goniometer into a mono-mode optical fiber (LPC-03-633-4/125-S-2-10AC-40-3S-3-2; OZ-Optics) with a core diameter of 4/125 mm which was connected to the photomultiplier. The remaining light was captured by a CCD camera (Allied Vision Tech, Stingray F-145B) for multi-speckle analysis. The intermediate scattering functions were calculated from the intensity correlation functions using three different methods, depending on the degree of ergodicity of the sample. The Siegert relation was used in the case of fully ergodic (fluid) samples to obtain $f(q, \tau)$. The intensity correlation function of non-ergodic samples was converted into $f(q, \tau)$ using the well known Pusey–van Meegen method (PvM) [26], which connects the ensemble average of $f(q, \tau)$ to the time-average of $g_T^{(2)}(q, \tau)$ via

$$f(q, \tau) = 1 + \frac{I_T}{I_E} \left\{ \left[g_T^{(2)}(q, \tau) - g_T^{(2)}(q, 0) \right]^{1/2} - 1 \right\} \quad (5)$$

I_T is the time average of the intensity recorded during a DLS measurement. I_E is the ensemble averaged intensity of the slowly rotated sample (about 1/60 s⁻¹) measured over a time interval of 300 s. In the glass transition range, where the PvM-method does no longer provide reliable data for long delay times τ [27,28], the multi-speckle approach was used. A CCD-camera acts as multi-detector system and allows for simultaneous monitoring of a large

number of speckles (in our case 2000) at the same scattering vector q . Using the collected intensity data, the ensemble averaged time correlation function $g_E^{(2)}(q, \tau)$ is calculated [27,28]. After applying the Siegert relation, $f(q, \tau)$ is obtained. Only delay times of $\tau \geq 0.5$ s were accessible due to the frame rate of the camera (2 s^{-1}). Delay times below this limit were gathered from a simultaneous standard DLS measurement, which was analyzed using the Siegert relation or the PvM method depending on the degree of nonergodicity of the samples. The data from the multi-speckle experiment were then normalized to the DLS data at $\tau = 1$ s. Generally a very good agreement of line shapes from both DLS and multispeckle method was found in an overlap region of $1 \text{ s} \leq \tau \leq 10 \text{ s}$. The typical sampling time was 24 h for both ergodic and non-ergodic samples.

2.2. Sample preparation

Two batches of polystyrene microgels were synthesized by emulsion polymerization with a cross-linking ratio of 1:10 using 1,3-diisopropenylbenzene as cross-linker. The particle sizes in aqueous suspension were obtained with dynamic light scattering (DLS) as $R_{H,H_2O,L} = 138 \pm 2 \text{ nm}$ and $R_{H,H_2O,S} = 115 \pm 2 \text{ nm}$ and with static light scattering (SLS) as $R_{SLS,H_2O,L} = 137 \pm 2 \text{ nm}$ and $R_{SLS,H_2O,S} = 117 \pm 2 \text{ nm}$ (S =small particles; L =large particles), the latter also providing the size polydispersity $\sigma_R = ((\langle r^2 \rangle) - \langle R \rangle^2)^{1/2} / \langle R \rangle = 0.06$ for both batches. The aqueous suspensions were then purified and dried as previously described [19]. The particle sizes and the polydispersities in dried state were measured with transmission electron microscopy (TEM), giving $R_{TEM,L} = 122 \pm 3 \text{ nm}$ ($\sigma_R = 0.05$) and $R_{TEM,S} = 113 \pm 3 \text{ nm}$ ($\sigma_R = 0.05$). In a good solvent the particle radius for a particle with a cross-linking ratio of 1:10 increases by a factor of $Q^{1/3} \approx 1.3$, where Q is the volume swelling ration. However, the radius of the swollen particles determined by DLS is inaccurate. This is due to the unaccounted influence of the permeability (controlled by the cross-linking ratio) of the particles on the hydrodynamic interactions, when using the Stokes–Einstein-equation to calculate the radius from the diffusion coefficient obtained with DLS [25]. To obtain the swelling ratio and from that a reasonably accurate radius of the particles in the good, iso-refractive solvent 2-ethylnaphthalene (2-EN; refractive index $n_D = 1.599$ [17,18,29]), the fluid–crystal coexistence of both batches in 2-EN was examined. The weight fractions of freezing and melting were determined by observing a set of samples over a course of a few months following literature procedures [19,30]. The volume fraction of the freezing point was assumed to be equal to that of hard spheres ($\phi_f = 0.494$ [31]), thereby ignoring the small effect of size polydispersity on the location of the freezing transition [32] as is been usually done when setting the volume fraction scale. Using

$$\phi = \frac{(w/d_p) \cdot Q_{HS}}{(w/d_p) + (1-w)/d_s} \quad (6)$$

where $d_p = 1.05 \text{ g/cm}^3$ and $d_s = 0.992 \text{ g/cm}^3$ are the mass densities of polystyrene and 2-EN, respectively, the swelling factor Q_{HS} was then calculated. Using $R_{HS} = Q^{1/3} \cdot R_{H,H_2O}$, the particle radii were calculated to be $R_{HS,L} = 184 \pm 2 \text{ nm}$ and $R_{HS,S} = 150 \pm 2 \text{ nm}$ which are identical of the particle sizes of the previously studied 1:50 cross-linked PS microgels within experimental accuracy. A stock solution of a binary mixture was prepared by weighing in the two particle systems yielding the size ratio of $R_{small}/R_{large} = 0.82$ and the same number ratio of $N = N_S/N_L = 2.7$ in 2-EN as used in an earlier study [16–18]. Ultrasonification was applied to the stock solution ($3 \times 15 \text{ min}$, Bandelin, Sonorex Super RK255H) to dissolve potential clusters of aggregated clusters that were previously observed with DLS in diluted suspension as a results of the freeze-drying procedure used for particle purification. Even longer exposure to ultrasound had no observable damaging effect

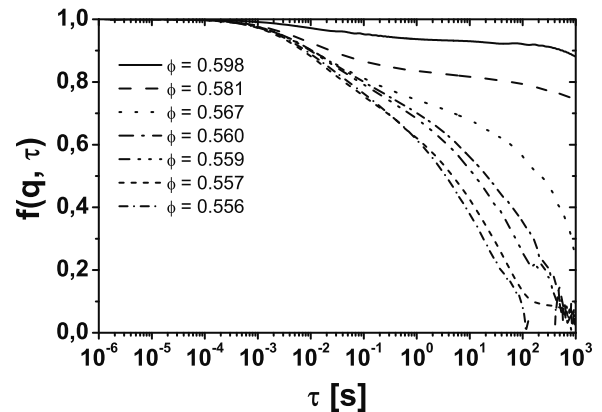


Fig. 1. Density auto-correlation function for the binary mixture of 1:10 cross-linked PS-particles ($R_L = 184 \text{ nm}$, $R_S = 150 \text{ nm}$) at the maximum of the static structure peak $q_{max} = 0.0255 \text{ nm}^{-1}$.

on the particles, as confirmed with DLS on diluted dispersions. To induce attractive depletion interactions among the microgel particles, dry polystyrene was added (Polymer Standards Service GmbH, Mainz, Germany, $M_W = 133,000 \text{ g/mol}$, $R_g = 12.6 \text{ nm}$, $M_W/M_N = 1.07$, $c_p^* = 3M_W/(4\pi N_A R_g^3) = 26.6 \text{ g/l}$ in toluene at ambient temperature; c_p^* = overlap concentration) as non-adsorbing polymer, resulting in range of the depletion attraction of $\xi \approx R_g/R_{binMix} = 0.078$, where R_{binMix} is the number-averaged particle radius of the mixture. 2-EN was then added to adjust the volume fraction ϕ , which was calculated using

$$\phi = \frac{\sum_i (m_i/d_p) \cdot Q_i}{\sum_i (Q_i/d_p) + m_s/d_s} \quad (7)$$

with the masses m_i of the PS-components $i = S, L, p$ (free polymer), m_s as the mass of the solvent and the swelling factor $Q_i = Q_{HS,L}$, $Q_{HS,S}$ and 0 for the free polymer. After addition of the free polymer or dilution of a stock suspension to the target concentration, the samples were tumbled (IKA Labortechnik: Janke&Kunkel, VF2) for at least 30 min for mixing, after which they were stored on a rotating wheel (Bibby Sterilin Ltd., Stuart Rotator SB2) for at least 3 days. The samples were centrifuged for 5 min at 1000 rpm to accumulate the suspension on the bottom of the cuvette for measurement and were then left for 20–30 min in order to relax any shear induced structures that might have been created by centrifugation.

3. Results and discussion

3.1. Glass transition

The glass transition of the binary mixture was determined by analyzing the dependence of the structural relaxation time τ_α in the vicinity of the glass transition. According to mode coupling theory [4] τ_α , defined as the time at which $f(q, \tau)$ has decayed to 0.3, should diverge with the power law [5,33]

$$\tau_\alpha = \tau_0 \left(1 - \frac{\phi}{\phi_g} \right)^{-\gamma} \quad (8)$$

on approaching the glass transition from the fluid side. The structural relaxation time was gathered from measurements displayed in Fig. 1. Using the HS value $\gamma = 2.5$, which has been shown to describe experimental data on HS colloids quite well [2,3] the MCT glass transition volume fraction was extracted via a rectification plot as shown in Fig. 2.

From the intersection of a linear regression line with the abscissa we obtained the glass transition of the binary mixture as $\phi_g = 0.564 \pm 0.005$. The shift of the glass transition to lower volume

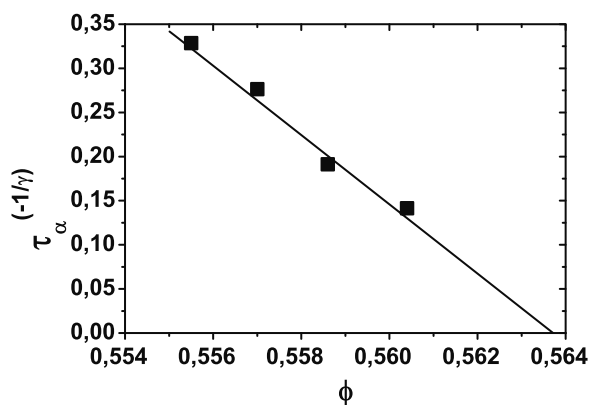


Fig. 2. Rectification plot of the volume fraction dependence of the structural relaxation time (Eq. (8)). τ_α was defined by $f(q, \tau) = 0.3$ and the HS value γ was used to obtain $\phi_g = 0.564$ by the intersection of the linear fit (solid line) with the abscissa.

fractions as compared to earlier studies on PS microgels, where glass transitions were found at volume fractions of $\phi_g = 0.584$ and $\phi_g = 0.595$ [17,19], is quite significant. However, for PMMA particles the glass transition was found at $\phi_g = 0.56$ – 0.578 [1,15,34]. Thus, the difference between the 1:10 and the 1:50 cross-linked particles might be, in principle, related to the hardness of the former particles, but with the large range of ϕ_g values found for HS PMMA particles, this shift could be coincidental.

3.2. Re-entry behavior of microgel systems with weak attractive interactions

To compare the effects of increasing the cross-linking ratio from 1:50 to 1:10 on the re-entrant melting behavior of microgels, we added a non-adsorbing depletion agent to the 1:10 cross-linked microgel dispersions. Using the earlier work as guideline, polymer concentrations up to $c_p = 8$ g/l were weighed in. The sample dynamics were analyzed by dynamic light scattering. Due to the long measurement times needed to determine one density correlation function and the huge number of samples close to an arrest line needed to accurately fix the transition point at a given colloid volume fraction by use of the power laws of MCT we refrained from employing this procedure. Instead we utilized a simpler approach by characterizing sample as fluid or glassy according to the intercept of $g^{(2)}(q, \tau)$ typically averaged over three measurements [17]. Samples with a $g^{(2)}(q, 0)$ of around 1.95 ± 0.02 were classified as ergodic, while samples with an intercept of 1.75 ± 0.5 or below were considered to be non-ergodic (see Fig. 3). Samples in-between that range were judged to be in the transition range.

The thus generated phase diagram is shown in Fig. 4. In order to eliminate the effect of the slight, but non negligible differences in glass transition volume fractions between different systems, the relative distance from the glass transition, $\epsilon = (\phi - \phi_g)/\phi_g$ is used instead of the colloid volume fraction. For the same reason the polymer concentration is converted into the polymer concentration in the free volume left by the colloidal particles, c_p^{free} , using the framework of scaled particle theory [35]. To make a connection between both scales the cut through the phase diagram shown in Fig. 3 is indicated by a straight dotted line in Fig. 4. As can be seen, the large re-entry region of the 1:50 cross-linked particles could not be reproduced with the more strongly cross-linked particles.

Whereas the glass transition and, thus, the fluid region is shifted up to about 18% (corresponding to a maximum volume fraction of about 0.69 at a polymer concentration of $c_p \approx 8$ g/l) for the 1:50 microgels, the re-entry effect is much weaker for the 1:10 microgel colloids amounting to a maximum shift of 8% (corresponding to a volume fraction of 0.61 at a polymer concentration of $c_p \approx 1.8$ g/l).

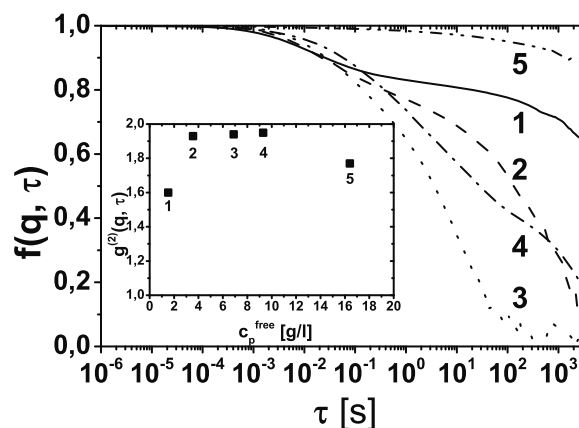


Fig. 3. Density correlation function for samples approximately constant volume fraction and increasing attraction strength (increasing concentration of polymer): 1: $\phi = 0.588$, $c_p = 0.410$ g/l; 2: $\phi = 0.588$, $c_p = 0.958$ g/l; 3: $\phi = 0.589$, $c_p = 1.858$ g/l; 4: $\phi = 0.588$, $c_p = 2.505$ g/l; 5: $\phi = 0.587$, $c_p = 4.451$ g/l. Inset: intercept of $g^{(2)}(q, \tau)$ for the same samples; samples with an intercept below 1.75 ± 0.5 were classified as non-ergodic, samples with $g^{(2)}(q, 0) \approx 1.95 \pm 0.02$ as ergodic.

In addition the polymer concentration needed to induce the attractive glass transition is significantly reduced for the 1:10 microgels as compared to the 1:50 ones. Close to the glass transition the polymer concentrations at the attractive glass transition differ by a factor of 5 in reduced units, corresponding to a change from $c_p = 15$ g/l (1:50) to 3 g/l (1:10) with respect to total sample volume. It is noticeable that the attractive glass line is now located at a c_p^{free} much lower than the overlap concentration c_p^* , in qualitative agreement with observations for the PMMA system. In contrast, the arrest of dynamics due to depletion attraction required polymer concentrations c_p^{free} about twice that of the overlap concentration ($c_p^* = 26.6$ g/l).

Fig. 5 compares the results for the 1:10 cross-linked microgel colloids with data taken from a work by Pham et al. [15] on PMMA particles dispersed in cis-decalin which can be assumed to be a good model system for hard spheres. In the latter case fluid states

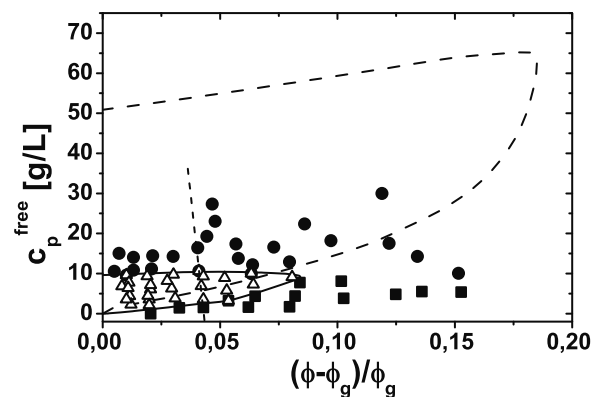


Fig. 4. Phase diagram of the binary mixture of 1:10 cross-linked particles as relative distance of the volume fraction from the glass transition volume fraction versus the polymer concentration in the free volume (left by the colloids). Squares denote samples in the repulsive glass, circles those in the attractive glass, open triangles indicate fluid states. Overlapping symbols of solid and open symbols indicate a sample in the transition region. The straight dotted line denotes the samples shown in Fig. 3. The solid line is a guide to the eye for the transition of the 1:10 cross-linked particles, the dashed line indicates the same for 1:50 cross-linked particles from an earlier study [18]. The overlap concentrations for the non-adsorbing polymer are $c_p^* = 26.6$ g/l and 27.6 g/l for the 1:10 and the 1:50 crosslinked microgel particles, respectively. The glass transition volume fraction were $\phi_g = 0.564$ and $\phi_g = 0.595$ for 1:10 and 1:50 crosslinked particles, respectively, and the polymer concentration with respect to total volume, c_p , were converted to polymer concentrations in the free volume, c_p^{free} within the framework of scaled particle theory (see Ilett et al. [35] for details).

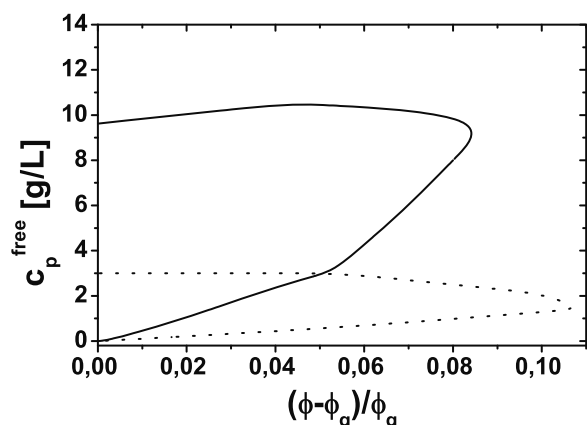


Fig. 5. Comparison of the re-entrant phase diagram of the 1:10 cross-linked particles (solid line) with data for PMMA-particles (dotted line) by Pham et al [15].

were observed up to volume fractions $\phi \approx 0.62$, i.e. up to slightly higher values than found for the 1:10 microgels.

Given the uncertainties in the exact location of the arrest transition lines, the differences of the criteria by which samples were assigned as fluid or glassy (in case of the PMMA particles the re-occurrence of crystallization was used to identify fluid samples) and the differences in particle size distribution (bimodal mixture in this work and monomodal PMMA dispersion) this discrepancy can be considered as rather insignificant. More pronounced is the difference in the amount of polymer needed in the free volume in order to induced an attraction driven arrest of the dynamics, i.e. an attractive glass transition. This different behavior may, however, be entirely due to polymer non-ideality in case of the microgel system. Here, the solvent 2-EN is a good solvent for PS so that excluded volume interactions come relevant for the free polymer whereas cis-decaline used for the PMMA particles is a nearly theta solvent, where such excluded volume interaction are negligible. An additional small effect that acts in the same direction might be the smaller attraction range $\xi = 0.078$ for the 1:10 microgels as compared to $\xi = 0.09$ for the PMMA particles [15]. Such a trend is well compatible with MCT predictions [10]. Thus, the 1:10 cross-linked microgels can be considered to behave as hard spheres to a good approximation even in the presence of free polymer. This is obviously not the case for the 1:50 crosslinked colloids. An obvious explanation for the high colloid volume fractions achieved for 1:50 microgels when free polymer is added is osmotic deswelling [20]. However, the crosslink density in the latter study was significantly lower as compared to the 1:50 microgels. In addition, an estimation of the PS segment density within the microgels and the PS segment density in the surrounding medium (due to free polymer) shows that the segment density inside the microgels is still so much higher than in the medium that no significant deswelling can be expected. Estimations based on data of macroscopic gels amount to an decrease of colloid volume fraction by about 2% even at the highest ϕ . This is not sufficient to explain the enormous re-entry effect of the 1:50 particles shown in Fig. 4 in comparison to the 1:10 particles. Additional effects must play a role.

A manifest explanation could be the transient deformation of the softer spheres under the influence of the depletion attraction. This would increase the free volume available to particle movement without increasing the polymer concentration inside of the PS microgels.

However, at present the complex interplay of cross-link density, polymer non-ideality and particle size distribution is not understood. Further experiments, involving a further variation of the system parameters like cross-link density, particle size distribution and polymer size are in progress. These are to be complemented by

determination of the particle form factor in such colloid polymer mixtures by small angle neutron scattering with contrast variation techniques.

4. Conclusion

We studied highly cross-linked (1:10) PS microgel particles at volume fractions ϕ above the glass transition volume fraction ϕ_g under the influence of depletion attraction to map the re-entrant melting region using DLS. In contrast to previous findings of fluid states up to a volume fraction of ≈ 0.69 due to polymer-induced re-entrant melting in case of (more softer) 1:50 crosslinked PS microgels we observe fluid states only up to $\phi \approx 0.61$. This significantly smaller re-entry effect of $\approx 8\%$ maximum shift of the colloid glass transition as compared to the huge 18% effect for 1:50 particles is in qualitative agreement with the behavior of PMMA hard sphere colloids. The much larger amount of free polymer required to reach the attractive glass transition in 1:10 microgels as compared to PMMA case can most likely be attributed to polymer non-ideality in the microgel case. The unexpectedly strong re-entry effect in the 1:50 microgels can probably be explained by a deformation of the softer 1:50 particles under the influence of the osmotic pressure, while a de-swelling of the particles seems to be unlikely. Further experiments with variation of system parameters like cross-link density, free polymer size and particle size distribution are under way to get a better understanding of the re-entry effect in PS microgel–PS polymer mixtures.

Acknowledgements

H. Moschallski is thanked for the synthesis of particles. The financial support by the German Research Foundation DFG within the priority program (SPP) 1273 is gratefully acknowledged.

References

- [1] W. van Meegen, P.N. Pusey, Dynamic light-scattering study of the glass transition in a colloidal suspension, *Phys. Rev. A* 43 (1991) 5429–5441.
- [2] W. van Meegen, S.M. Underwood, Glass transition in colloidal hard spheres: measurement and mode-coupling-theory analysis of the coherent intermediate scattering function, *Phys. Rev. E* 49 (1994) 4206–4220.
- [3] W. van Meegen, T.C. Mortensen, S.R. Williams, J. Müller, Measurement of the self-intermediate scattering function of suspensions of hard spherical particles near the glass transition, *Phys. Rev. E* 58 (1998) 6073–6085.
- [4] W. Götze, Aspects of structural glass transitions, in: *Liquids, Freezing and the Glass Transition*, North-Holland, Amsterdam, 1991.
- [5] W. Götze, L. Sjögren, β relaxation at the glass transition of hard-spherical colloids, *Phys. Rev. A* 43 (1991) 5442–5448.
- [6] L. Fabbian, W. Götze, F. Sciortino, P. Tartaglia, F. Thiery, Ideal glass–glass transitions and logarithmic decay of correlations in a simple system, *Phys. Rev. E* 59 (1999) R1347–R1350.
- [7] W. van Meegen, S.R. Williams, Comment on probing the equilibrium dynamics of colloidal hard spheres above the mode-coupling glass transition, *Phys. Rev. Lett.* 104 (2010) 169601.
- [8] G. Brambilla, D. El Masri, M. Pierno, L. Berthier, L. Cipelletti, G. Petekidis, A. Schofield, Brambilla et al. reply, *Phys. Rev. Lett.* 104 (2010) 169602.
- [9] L. Fabbian, W. Götze, F. Sciortino, P. Tartaglia, F. Thiery, Erratum ideal glass–glass transitions and logarithmic decay of correlations in a simple system (*Phys. Rev. E* 59 (1999) r1347), *Phys. Rev. E* 60 (1999) 2430.
- [10] K. Dawson, G. Foffi, M. Fuchs, W. Götze, F. Sciortino, M. Sperl, P. Tartaglia, T. Voigtmann, E. Zaccarelli, Higher-order glass-transition singularities in colloidal systems with attractive interactions, *Phys. Rev. E* 63 (2000) 011401.
- [11] F. Oosawa, S. Asakura, Surface tension of high polymer solutions, *J. Chem. Phys.* 22 (1954) 1255.
- [12] S. Asakura, F. Oosawa, Interaction between particles suspended in solutions of macromolecules, *J. Polym. Sci.* 33 (1958) 183–192.
- [13] A. Vrij, Polymers at interfaces and the interactions in colloidal dispersions, *Pure Appl. Chem.* 48 (1976) 471–483.
- [14] K.N. Pham, A.M. Puertas, J. Bergenholtz, S.U. Egelhaaf, A. Moussaïd, P.N. Pusey, A.B. Schofield, M.E. Cates, M. Fuchs, W.C.K. Poon, Multiple glassy states in a simple model system, *Science* 296 (2002) 104–106.
- [15] K.N. Pham, S.U. Egelhaaf, P.N. Pusey, W.C.K. Poon, Glasses in hard spheres with short-range attraction, *Phys. Rev. E* 69 (2004) 011503.
- [16] T. Eckert, E. Bartsch, Re-entrant glass transition in a colloid–polymer mixture with depletion attractions, *Phys. Rev. Lett.* 89 (2002) 125701.

- [17] T. Eckert, E. Bartsch, The effect of free polymer on the interactions and the glass transition dynamics of microgel colloids, *Faraday Discuss.* 123 (2003) 51–64.
- [18] T. Eckert, E. Bartsch, Glass transition dynamics of hard sphere like microgel colloids with short-ranged attractions, *J. Phys.: Condens. Matter* 16 (2004) S4937.
- [19] N. Willenbacher, J.S. Vesaratchanon, O. Thorwarth, E. Bartsch, An alternative route to highly concentrated, freely flowing colloidal dispersions, *Soft Matter* 7 (2011) 5777–5788.
- [20] B. Saunders, B. Vincent, Osmotic de-swelling of polystyrene microgel particles, *Colloid Polym. Sci.* 275 (1997) 9–17.
- [21] W. Schärtl, H. Sillescu, Brownian dynamics of polydisperse colloidal hard spheres: equilibrium structures and random close packings, *J. Stat. Phys.* 77 (1994) 1007–1025.
- [22] B. Berne, R. Pecora, *Dynamic Light Scattering. With Applications to Chemistry, Biology, and Physics*, Wiley-Interscience, New York, NY, USA, 1976.
- [23] B. Chu, *Laser Light Scattering: Basic Principles and Practice*, Academic Press, Boston, 1991.
- [24] D.E. Koppel, Analysis of macromolecular polydispersity in intensity correlation spectroscopy: the method of cumulants, *J. Chem. Phys.* 57 (1972) 4814–4820.
- [25] G.C. Abade, B. Cichocki, M.L. Ekiel-Jeżewska, G. Nägele, E. Wajnryb, Short-time dynamics of permeable particles in concentrated suspensions, *J. Chem. Phys.* 132 (2010) 014503.
- [26] P. Pusey, W. van Meegen, Dynamic light scattering by non-ergodic media, *Physica A* 157 (1989) 705–741.
- [27] E. Bartsch, V. Frenz, S. Kirsch, W. Schärtl, H. Sillescu, Multi-speckle autocorrelation spectroscopy – a new strategy to monitor ultraslow dynamics in dense and nonergodic media, in: T. Palberg, M. Ballauff (Eds.), in: *Optical Methods and Physics of Colloidal Dispersions*, Progress in Colloid and Polymer Science, vol. 104, Springer, Berlin, Heidelberg, 1997, pp. 40–48, doi:10.1007/BFb0110743.
- [28] E. Bartsch, V. Frenz, J. Baschnagel, W. Schärtl, H. Sillescu, The glass transition dynamics of polymer microneutral network colloids, a mode coupling analysis, *J. Chem. Phys.* 106 (1997) 3743–3756.
- [29] S.E. Paulin, B.J. Ackerson, Observation of a phase transition in the sedimentation velocity of hard spheres, *Phys. Rev. Lett.* 64 (1990) 2663–2666.
- [30] H. Senff, W. Richtering, Temperature sensitive microgel suspensions: colloidal phase behavior and rheology of soft spheres, *J. Chem. Phys.* 111 (1999) 1705–1711.
- [31] P.N. Pusey, W. van Meegen, Phase behaviour of concentrated suspensions of nearly hard colloidal spheres, *Nature* 320 (1986) 340–342.
- [32] M. Fasolo, P. Sollich, Fractionation effects in phase equilibria of polydisperse hard-sphere colloids, *Phys. Rev. E* 70 (2004) 041410.
- [33] W. Götze, Recent tests of the mode-coupling theory for glassy dynamics, *J. Phys.: Condens. Matter* 11 (1999) A1.
- [34] S. Henderson, T. Mortensen, S. Underwood, W. van Meegen, Effect of particle size distribution on crystallisation and the glass transition of hard sphere colloids, *Phys. A: Stat. Mech. Appl.* 233 (1996) 102–116.
- [35] S.M. Ilett, A. Orrock, W.C.K. Poon, P.N. Pusey, Phase behavior of a model colloid–polymer mixture, *Phys. Rev. E* 51 (1995) 1344–1352.